# Surface Integral Computation for the Higher Order Surface Integral Equation Method of Moments

Sanja B. Manić and Branislav M. Notaroš Department of Electrical and Computer Engineering Colorado State University Fort Collins, Colorado, USA smanic@colostate.edu, notaros@colostate.edu

Abstract—This paper presents extraction technique applied to the double higher order surface integral equation method of moments and discusses the numerical results compared with previously implemented extraction method and numerical Gauss-Legendre integration.

Keywords— double higher order method of moments, integral accuracy, integration extraction technique, surface integral equation.

### I. INTRODUCTION

This paper presents our ongoing study of convergence behavior of near-singular (potential) and near-hypersingual (field) integrals for double higher order large-domain surface integral equation method of moments (SIE-MoM). The fast and accurate integral computation that will effectively give the MoM matrix entries is essential in the computational electromagnetics (CEM). The challenge arises with small source-to-field distances which often occur in microstrip and printed circuit design but are part of almost any model analysis. The technique for integral evaluation presented here uses the singularity extraction method. The analytically evaluated integral of the principal singular part is computed over a parallelogram which surface is defined to be similar to the surface of the generalized quadrilateral in the near area of the singular point. Numerical integrals over parallelogram and quadrilateral are using Gauss-Legendre quadrature formula.

### II. THE METHOD

# A. 2D Double Higher Order Integrals

In the double higher order SIE-MoM the 2D surface integrals are defined on the Lagrange-type generalized curved parametric quadrilateral MoM-SIE surface elements (in Fig. 1) defined in the parametric *u-v* domain as [1]:

$$\mathbf{r}(u,v) = \sum_{k=0}^{K_u} \sum_{l=0}^{K_v} \mathbf{r}_{kl} u^k v^l , \text{ for } -1 \le u, v \le 1,$$
 (1)

where  $\mathbf{r}_{kl}$  are vector coefficients and  $K_u$  and  $K_v$  are geometrical orders ( $K_u$ ,  $K_v \ge 1$ ). The current is approximated by higher order polynomial basis functions [1] leading to 2D integrals over the quadrilateral having the following form:

$$I_{ij}^{s} = \int_{-1}^{1} \int_{-1}^{1} \frac{u^{i} v^{j} e^{-i\beta R}}{4\pi R} du dv, \quad I_{ij}^{hs} = \int_{-1}^{1} \int_{-1}^{1} \frac{u^{i} v^{j} (1 + j\beta R) e^{-j\beta R}}{4\pi R^{3}} du dv, \quad (2)$$

where s and hs represent singular and hypersingular integrals respectively, i and j are arbitrary polynomial orders

of the basis functions,  $\beta = 2\pi f \sqrt{\epsilon \mu}$ , f is the operating frequency,  $\epsilon$  and  $\mu$  are permittivity and permeability of the dielectric medium respectively and R is the distance of the source point from the field point.

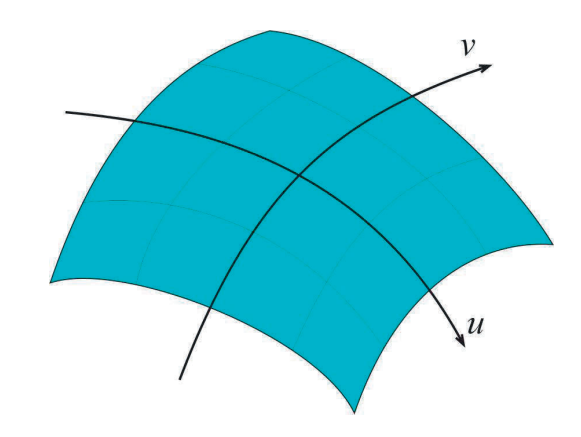


Fig. 1. Quadrilateral element.

# B. Defining the Paralelogram for the Extraction Technique

The quadrilateral element and the parallelogram constructed at projection point  $(u_0, v_0)$  are shown in Fig. 2. The distance of the point on the parallelogram and singular point is defined as:

$$R_p^2 = d^2 + a_u^2 \Delta u^2 + a_v^2 \Delta v^2 + 2a_u a_v \cos \alpha \Delta u \Delta v , \qquad (3)$$

where  $a_u$ ,  $a_v$  and  $\cos \alpha$  are computed to take into account the curvature of the quadrilateral element,  $\Delta u = u - u_0$ ,  $\Delta v = v - v_0$  and d is the distance between singular point and the close point projection on the quadrilateral element.

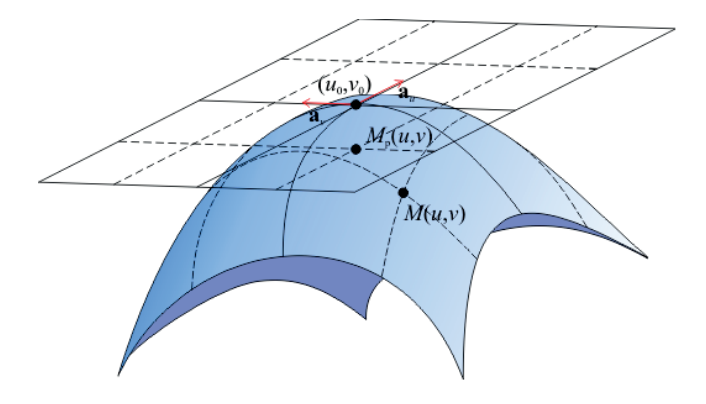


Fig. 2. Quadrilateral patch and parallelogram constructed at projected point.

# C. Taylor's Expantion and Analytical Integration

The relation between quadrilateral and parallelogram parametric surfaces is given by:

 $R(u,v)^2 = R_p^2(u,v) + t(u,v)$ ,  $R(u,v) = R_p \sqrt{1 + x(u,v)}$ , (4) where  $x(u,v) = t(u,v)/R_p^2(u,v)$ . The singular and hypersingular parts of integrands for the integration over the parallelogram are represented through Taylor's expansion over x having in mind (4). Analytical integrals are computed by dividing parallelogram into triangles and using recursive formulas similarly to the procedure described in [2].

# D. Projected Points Outside of the Patch

For the case of large and negative  $2a_ua_v\cos\alpha\Delta u\Delta v$  contribution in (3), |x(u,v)| becomes large because  $R_p^2(u,v)$  is taking a small value. As a result, the Taylor's expansion over x does not approximate the (hyper) singular function well. In this situation, when the projection point is outside of the element domain, the parallelogram is constructed using parameters at the closest point, i.e. the most singular point on the quadrilateral. For the large values of |x(u,v)|, the patch is divided into four parts and the extraction method is applied to each part separately (example in Fig. 5).

# III. RESULTS

The results shown in this section are computed for second order curvilinear patch (one of the six patches modeling 1 m radius sphere) shown in Fig. 2. The integral convergence is obtained for d=5e-7 and  $\beta$  = 0.775462658083873 and results are compared to Gauss-Legendre numerical integration and previously implemented traditional (old) extraction technique.

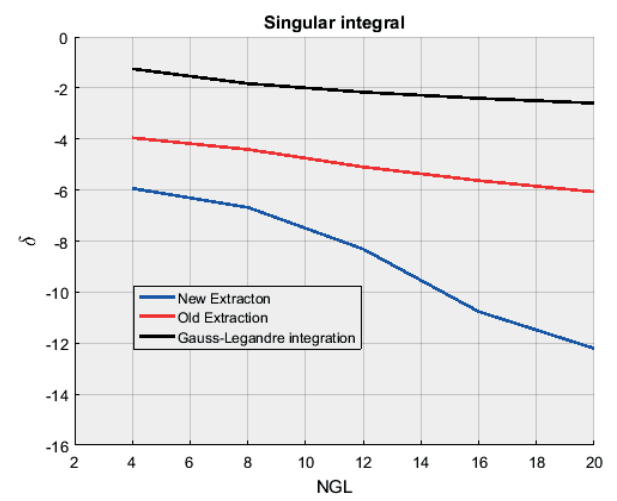


Fig. 3. Singular integral convergence for  $u_0 = 0.1$ ,  $v_0$ =-0.1 (the projection point) and i=0, j=0 orders of the basis function.

The NGL label on the graphs represents the square root of the number of Gauss-Legendre points used for the numerical integration over quadrilateral or parallelogram. The relative convergence error is computed as  $\delta = \log_{10} \left| I - \widetilde{I} \right| / \left| \widetilde{I} \right|$ , where  $\widetilde{I}$  is the integral computed using described extraction method with high value of Gauss-Legendre points and I represents the integrals as function of NGL.

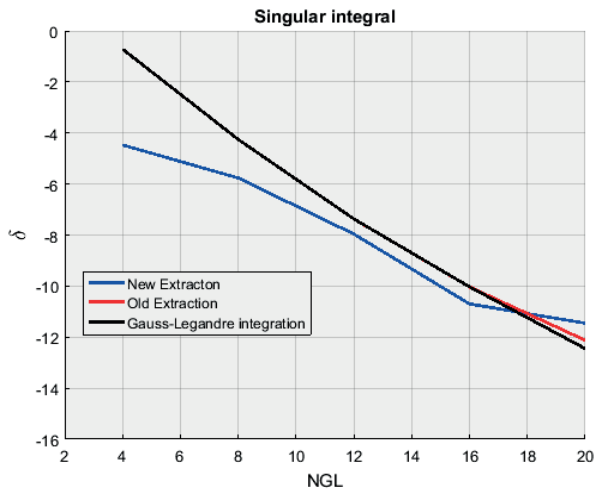


Fig. 4. Singular integral convergence for  $u_0 = 0.1$ ,  $v_0$ =-0.1 (the projection point) and i=6, j=6 orders of the basis function.

Results in Fig. 5 are computed for the point described in part D of previous section and the improvement in convergence is shown for the divided patch method.

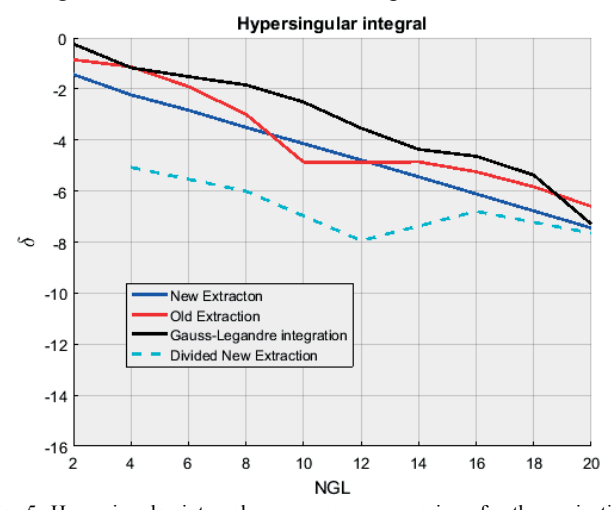


Fig. 5. Hypersingular integral convergence comparison for the projection point  $u_0 = 1.1$ ,  $v_0=1.1$  and i=0, j=0 orders of the basis function. Patch is divided at (0.8, 0.8) point in u-v domain.

# IV. CONCLUSION

New extraction method is introduced and the method is verified with results. The convergence improvement is shown compared to the traditional extraction technique as well as further improvements achieved by dividing the patch. The convergence improvement is due the integral of the difference of the two functions defined over the constructed parallelogram and quadrilateral being accurately evaluated with small number of integration points.

### REFERENCES

- [1] M. Djordjevic and B. M. Notaros, "Double higher order method of moments for surface integral equation modeling of metallic and dielectric antennas and scatterers," IEEE Transactions on Antennas and Propagation, vol. 52, no. 8, pp. 2118-2129, August 2004.
- [2] S. Jarvenpaa, M. Taskinen, and P. Yla-Oijala, "Singularity subtraction technique for high-order polynomial vector basis functions on planar triangles," IEEE Transactions on Antennas and Propagation, vol. 54, no. 1, pp. 42-49, January 2006.